Progress of Theoretical Physics, Vol. 67, No. 6, June 1982

Periodic Spinodal Decomposition in Solid Binary Mixtures

Akira ONUKI

Department of Physics, Kyushu University, Fukuoka 812

(Received January 16, 1982)

Phase separation is studied when the temperature is made to oscillate around a critical value near a second-order phase transition. In such a case the structure factor is calculated for a one-component system with conserved order parameter using a computational method of Langer, Bar-on and Miller. The structure factor tends to a periodic function when the average of the oscillating temperature is higher than a new critical value which is lower than the equilibrium critical temperature. However, its maximum grows without limit when the average temperature is lowered below the critical value. This is a new type of phase transition where the fluctuations are much enhanced above the thermal level. Besides solid binary mixtures the results of this paper are applicable to uniaxial ferromagnets under strong ultrasounds in which the spin component along the easy axis is conserved.

§ 1. Introduction

Systems in the neighborhood of a second-order phase transition can undergo periodic spinodal decomposition if the temperature T is made to oscillate around the critical temperature T_c.[1)~4)] If the oscillation is sufficiently slow, domains (or clusters) can be formed periodically since the phase separation proceeds while $T < T_c$. If the decay mechanism of domains which is effective while $T > T_c$ is strong enough, the phase separation will be stopped and then the domain sizes will remain finite. In such a case the system is in a disordered phase on a length scale much greater than the size of characteristic domains and will behave periodically after a long time. However, if the average temperature is lowered below a certain value, domains can be only partially dissipated while $T > T_c$ and will continue to grow up to the system size. This means that there should be a phase transition as the average temperature is lowered with a fixed size of the oscillation. This transition occurs when the decay mechanism becomes less effective than the formation mechanism.

Periodic spinodal decomposition may be realized by various methods. One is to make $T - T_c$ oscillate by ultrasounds.[1)] This method is suitable for systems where the ordering process takes place too quickly for usual measurements. Note that previous experimental works of the spinodal decomposition are limited to alloys, glassy mixtures, and fluid mixtures where the time scale is very slow. Therefore, periodic spinodal decomposition may provide us a potentially rich field of nonequilibrium physics, although it has drawn no attention so far.

In previous papers this phenomenon has been investigated in a one-com-

ponent system with nonconserved order parameter.[2),3)] In this paper it will be examined for the following model with a single-component, conserved order parameter $c(\boldsymbol{r}, t)$:[4)]

$$\frac{\partial}{\partial t}c=L\nabla^2\left[r(t)+r_{0c}-\nabla^2+\frac{1}{6}gc^2\right]c+\theta\,. \tag{1·1}$$

Here L is the kinetic coefficient, $r(t)$ is proportional to $T-T_c$ and is oscillating in time, r_{0c} is a shift of T_c due to the fluctuation effect, and $\theta(\boldsymbol{r}, t)$ is a Gaussian Markov noise related to L by

$$\langle\theta(\boldsymbol{r}, t)\theta(\boldsymbol{r}', t')\rangle=-2L\nabla^2\delta(\boldsymbol{r}-\boldsymbol{r}')\delta(t-t'). \tag{1·2}$$

The value of the coupling constant g will be given below (2·9). This model simulates solid binary mixtures, if the complicated effects of coherency strains are neglected,[5)~7)] and more precisely the spin-exchange, kinetic Ising model used in computer simulations.[8)] In these systems the temperature will be easily made to oscillate. The model (1·1) may also describe uniaxial ferromagnets under strong ultrasounds in which the component of the spin along the easy axis is a conserved order parameter.[9)]

We assume that $r(t)$ is undergoing a step-wise oscillation,

$$r(t)=r_1\sigma+r_1F(t/t_p), \tag{1·3}$$

where $r_1(>0)$ is the amplitude of the oscillation, $r_1\sigma$ is the average, and $F(x)$ is a periodic function being equal to -1 for $n\leq x<n+1/2$ and to 1 for $n+1/2\leq x<n+1$ with n integral values. Thus t_p is the period of the oscillation. This type of oscillation will be easily realized in experiments.

For $\sigma>1$, we have $T>T_c$ at any time and nothing particular can be expected. For $\sigma<-1$ the phase separation cannot be interrupted.*) The case $|\sigma|<1$ is a new unexplored situation, where the formation and decay mechanisms of domains can compete. Here we consider the problem at the critical composition. The frequency scale of the growing fluctuations is $L\,k_c^4$ with

$$k_c=r_1^{1/2}\,. \tag{1·4}$$

Note that the growing rate of $\tilde{S}_k(t)$ takes the maximum $\frac{1}{4}Lk_c^4$ at $k=2^{-1/2}k_c$ when $r(t)=-r_1$ within the simple linear theory.[5)~7)] The fluctuations with wave numbers greater than k_c are not much affected, whereas those with wave numbers smaller than k_c can be much enhanced. The degree of the enhancement is represented by a dimensionless number μ defined by

$$\mu=Lk_c^4t_p\,. \tag{1·5}$$

*) In this case the system will separate into two phases. But we do not know the effects of the temperature vibration on the coexistence curve. This aspect of the problem must also be investigated in future work.

For $\mu \gg 1$ strong enhancement occurs, whereas for $\mu \ll 1$ the oscillation is too rapid for the cluster formation. However, long-wavelength fluctuations have time scales proportional to k^{-2} (where k is the wave number) and cannot change appreciably in one period. Therefore, if we observe only the first period, enhancement occurs only in an intermediate wave number region

$$\mu^{-1/2} k_c \lesssim k \lesssim k_c \,. \tag{1·6}$$

It should be noted that the long-wavelength fluctuations with $k \lesssim \mu^{-1/2} k_c$ can be enhanced after several periods if σ is lowered to negative values.*) This is because the clusters with wave numbers in the region (1·6) can develop into those with sizes greater than $\mu^{1/2} k_c^{-1}$ for negative σ.

In this paper we numerically follow the time-development of the structure factor $\tilde{S}_k(t)$ for various σ and μ on the basis of a computational method of Langer, Bar-on and Miller (LBM)[10] to confirm the physical pictures presented in this section. In § 2 the LBM scheme will be generalized to the periodic case and in § 3 numerical results will be presented together with their interpretation. In § 4 spinodal curves will be calculated in the presence of the oscillation.

§ 2. LBM scheme for peirodic quench

LBM devised a tractable computational method for the model (1·1) in the case of a sudden quench into unstable states (but we must rely on computer). They obtained a closed set of equations for $\tilde{S}_k(t)$ and the one-point distribution function

$$\rho_1(c_1, t) = \langle \delta(c(\boldsymbol{r}, t) - c_1) \rangle \tag{2·1}$$

by making an ansatz for the two-point distribution function

$$\rho_2(c_1, c_2; |\boldsymbol{r}_1 - \boldsymbol{r}_2|, t) = \langle \delta(c(\boldsymbol{r}_1, t) - c_1) \delta(c(\boldsymbol{r}_2, t) - c_2) \rangle. \tag{2·2}$$

The ansatz is expressed as

$$\begin{aligned} \rho_2(c_1, c_2; |\boldsymbol{r}_1 - \boldsymbol{r}_2|, t) &= \rho_1(c_1, t) \rho_1(c_2, t) \\ &\times [1 + \gamma(|\boldsymbol{r}_1 - \boldsymbol{r}_2|, t)(c_1 - c_0)(c_2 - c_0)], \end{aligned} \tag{2·3}$$

where c_0 is the average composition. Hereafter we introduce the deviation $u(\boldsymbol{r}, t)$ by

$$u(\boldsymbol{r}, t) = c(\boldsymbol{r}, t) - c_0 \,. \tag{2·4}$$

Then the pair correlation function is expressed as

*) In the linear theory where the nonlinear coupling among the fluctuations is neglected we cannot find that these long-wavelength fluctuations can be enhanced.[1]

$$\tilde{S}(r, t)=\langle u(\boldsymbol{r}, t)u(\boldsymbol{0}, t)\rangle=\langle u^2\rangle^2\gamma(r, t). \tag{2·5}$$

The Fourier transform of $\tilde{S}(r, t)$ is $\hat{S}_k(t)$. The ansatz (2·3) implies that any correlation functions of the form $\langle u^n(r, t)u^m(0, t)$ with n and m being odd integral values have the same spatial dependence as $\tilde{S}(r, t)$.

In our periodic case we also assume (2·3). In particular, the structure factor obeys

$$\frac{\partial}{\partial t}\hat{S}_k(t)=-2Lk^2[k^2+A(t)]\hat{S}_k(t)+2Lk^2\,, \tag{2·6}$$

where

$$A(t)=r(t)+r_{0c}+\frac{1}{6}g\langle(c_0+u)^3u\rangle/\langle u^2\rangle. \tag{2·7}$$

Other resultant equations can be found in the Appendix. Hereafter $u(\boldsymbol{r}, t)$ must be assumed to consist of Fourier components with wave numbers smaller than a cutoff $k_{\max}$. Since fluctuations with wave numbers much greater than k_c are insensitive to the quench, we may assume the relation

$$k_{\max}=\beta k_c \tag{2·8}$$

with β an adjustable parameter of order unity. Then $\langle u^2\rangle$ and $\hat{S}_k(t)$ are related by

$$\langle u^2\rangle=\frac{1}{2\pi^2}\int_0^{k_{\max}} dk\; k^2\hat{S}_k(t). \tag{2·9}$$

In our numerical analysis the ratio of the left-hand side to the right-hand side has been kept to be between 0.999 and 1.001. The dimensionless coupling constant $g^*\equiv g/k_c$ will be chosen as 21.8, which is an appropriate value for the kinetic Ising model.[11),12)] The constant r_{0c} is given by $-\frac{1}{6}\varepsilon k_{\max}^2$ slightly below four dimensions with $\varepsilon=4-d$, d being the spatial dimensionality, but we do not know its precise value at $d=3$.*) One possible choice is to determine r_{0c} such that $\hat{S}_k(t)$ grows indefinitely if r is fixed at a negative value and it tends to a limit $1/(k^2+A_\infty)$ if r is fixed at a positive value. Then we find numerically

$$r_{0c}=-0.374k_c{}^2 \tag{2·10}$$

using the LBM approximation with $\beta=1$ (see the Appendix). Generally, the magnitude of the coefficient in front of $k_c{}^2$ is an increasing function of β. In particular, it is 0.565 for $\beta=\sqrt{2}$.

It is convenient to rewrite the equations in terms of the following dimensionless wave number and time:

*) In the case of a single quench $k_{\max}$ should be chosen to be of the order of the inverse correlation length at the final temperature. Then r_{0c} is only an amplitude correction to r.

$$q=k/k_c, \qquad \tau=2Lk_c^4 t\,. \tag{2·11}$$

We also introduce a dimensionless order parameter y and a dimensionless structure factor $S(q,\tau)$ by

$$y=(g/6)^{1/2}k_c^{-1}u\,, \qquad S(q,\tau)=k_c^2\hat{S}_k(t). \tag{2·12}$$

The period of the oscillation is 2μ in the dimensionless units. Then, (2·6) becomes

$$\frac{\partial}{\partial\tau}S(q,\tau)=-q^2[q^2+a(\tau)]S(q,\tau)+q^2 \tag{2·13}$$

with

$$a(\tau)=\bar{\sigma}+F(\tau/2\mu)+\langle(x_0+y)^3y\rangle/\langle y^2\rangle\,, \tag{2·14}$$

where *)

$$\bar{\sigma}=\sigma+r_{0c}/k_c^2\,, \tag{2·15}$$

$$x_0=(g/6)^{1/2}k_c^{-1}c_0\,. \tag{2·16}$$

Note that $\bar{\sigma}=\sigma-0.374$ if (2·10) is assumed.

§ 3. Numerical results at the critical composition

In this section we report numerical results at the critical composition ($x_0=0$) by setting $\beta=1$. The initial conditions for most of the calculations are as follows:

$$S(q,0)=1/(q^2+1), \qquad b_1=b_2=0.1001, \qquad v=0.1715\,, \tag{3·1}$$

where b_1, b_2 and v are parameters in the definition of the one-point distribution function (A·6). These constitute a stationary state of the LBM model if $r+r_{0c}$ is fixed at $0.887r_1$ (see the Appendix). In LBM the quantities in (3·1) are assumed to be zero at $\tau=0$, which corresponds to a quench from a very high temperature. The effects of the initial conditions almost disappear after a short time interval except for very long-wave length fluctuations as long as (2·9) is satisfied at $\tau=0$. Therefore, the choice of the initial conditions is not important. See also sentences about a_∞ and σ_c below (3·3). We integrate (2·13), (A·7), (A·10), and (A·11) by the simplest difference method with the width of unit time intervals being equal to 0.2. Even if the width is chosen as 0.02, the numerical results coincide with those of 0.2 within a few percent. The wave number region $0\leq q\leq 1$ is divided into intervals with width 0.01.

In Fig. 1 we show the growth of $S(q,\tau)$ for $0\leq\tau\leq 60$ in the case of a single

*) In Ref. 4), $\bar{\sigma}$ is written as σ.

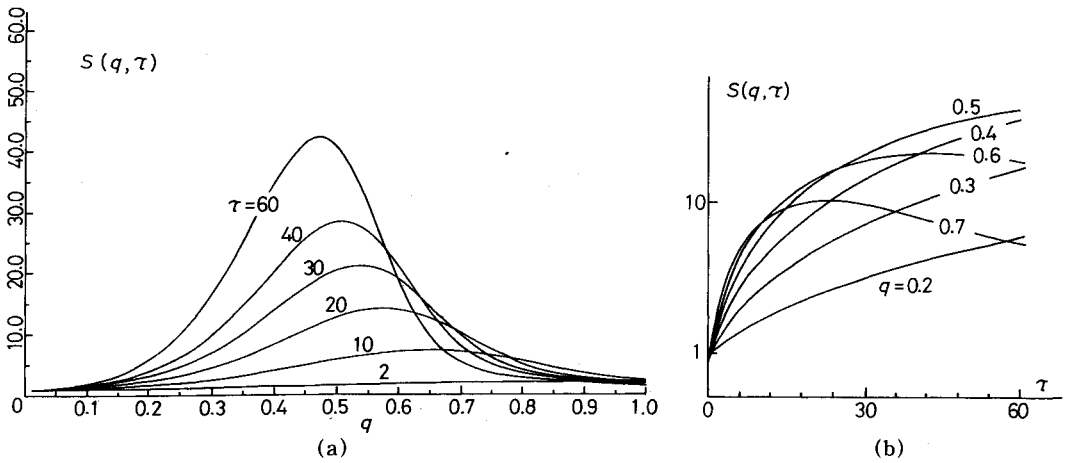

Fig. 1. (a) Growing of $S(q, \tau)$ after a quench at $\tau=0$. (b) $S(q, \tau)$ for $q=0.2, \cdots,$ 0.7 on a semi-log scale.

quench, $r+r_{0c}=-k_c^2$. The maximum of $S(q, 60)$ is 42.3, which is about twice larger than the corresponding value of LBM. This difference mainly comes from the choice of β. In fact, we performed the same calculation at $\beta=\sqrt{2}$ and $r+r_{0c}=-k_c^2$ and found the maximum value of $S(q, 60)$ to be 22.3. Next $r+r_{0c}$ is changed from $-k_c^2$ to k_c^2 suddenly at $\tau=60$. Then $S(q, \tau)$ decays almost exponentially as is shown in Fig. 2. In this case $a(\tau)$ tends to 1.11 as $\tau \to \infty$ (see the Appendix). This limit is reached within 1% for $\tau-60 \gtrsim 20$. In Fig. 2(c) we display the ratio of $S(q, \tau)$ to the following approximant:

$$S_A(q, \tau)=[S(q, 60)-1/(q^2+1.11)] \times \exp[-q^2(q^2+1.11)(\tau-60)]+1/(q^2+1.11), \tag{3·2}$$

which is the solution of (2·13) with $a=1.11$. We notice that $S(q, \tau)$ decays considerably faster than $S_A(q, \tau)$ for $\tau-60 \lesssim 10$. This is because $a(\tau)=1+\langle y^4\rangle/\langle y^2\rangle$ is appreciably greater than 1.11 for $\tau-60 \lesssim 10$, as can be known from Fig. 3. We may say within the LBM approximation that the relaxation of $S(q, \tau)$ toward the thermal Ornstein-Zernike form takes place much faster than the growth. This distinct difference of the two time scales results in a lowering of the critical temperature in the presence of the oscillation, since the formation and decay processes of the fluctuations can compete only for negative values of σ.

When the temperature is made to oscillate as (1·3), $S(q, \tau)$ grows and decays drastically in each period for $\mu \gg 1$. We find that $S(q, \tau)$ tends to behave periodically if σ is greater than a particular value σ_c, whereas the maximum of $S(q, \tau)$ grows indefinitely for $\sigma<\sigma_c$. Here the period 2μ is fixed and σ is varied. In Figs. 4 and 5 we plot the following average intensities at $\mu=20$ for $\sigma>\sigma_c$ and

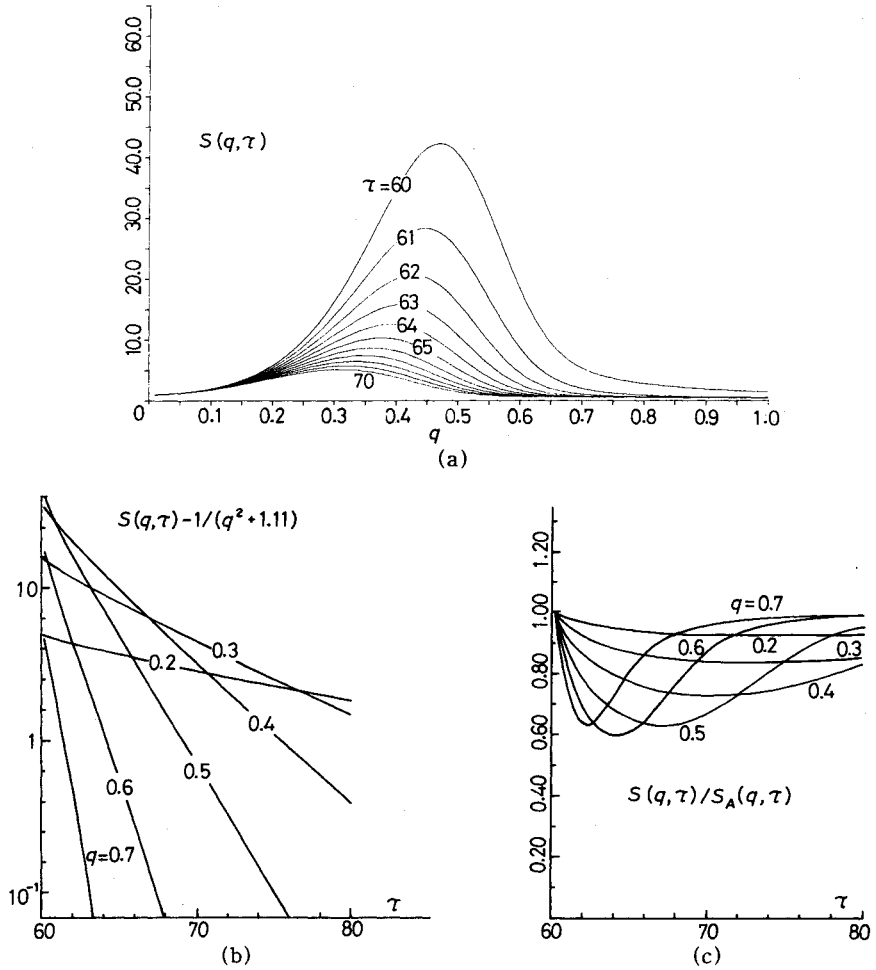

Fig. 2. (a) Relaxation of $S(q, \tau)$ after a reverse quench at $\tau=60$. (b) $S(q, \tau)-1/(q^2+1.11)$ for $q=0.2, \cdots, 0.7$ on a semi-log scale. (c) The ratio of $S(q, \tau)$ to $S_A(q, \tau)$ for $60<\tau<80$.

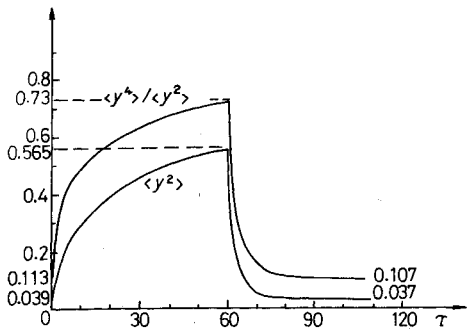

Fig. 3. Time-development of $\langle y^2\rangle$ and $\langle y^4\rangle/\langle y^2\rangle$. The initial conditions and the temperature are the same as in Figs. 1 and 2. The relaxation of these quantities after the reverse quench takes place quickly within the time interval of 20. At $\tau=0$ and ∞, the model is in stationary states and the ratio $\langle y^4\rangle/\langle y^2\rangle^2$ is close to the Gaussian value 3. This ratio decreases in the course of spinodal decomposition and becomes 1.29 at $\tau=60$.

$\sigma<\sigma_c$, respectively :

$$S_n(q)=\frac{1}{2\mu}\int_{2(n-1)\mu}^{2n\mu} d\tau S(q,\tau). \tag{3·3}$$

Interestingly, $S_n(q)$ have two peaks and $S(q,\tau)$ also have two peaks in some time regions. In Fig. 6 the maximum wave numbers and the maximum values of $S(q,\tau)$ are displayed at $\mu=20$ and $\bar{\sigma}=\sigma-0.374=-0.55$. These figures show that there are two types of clusters, as was argued in § 1. The smaller ones are

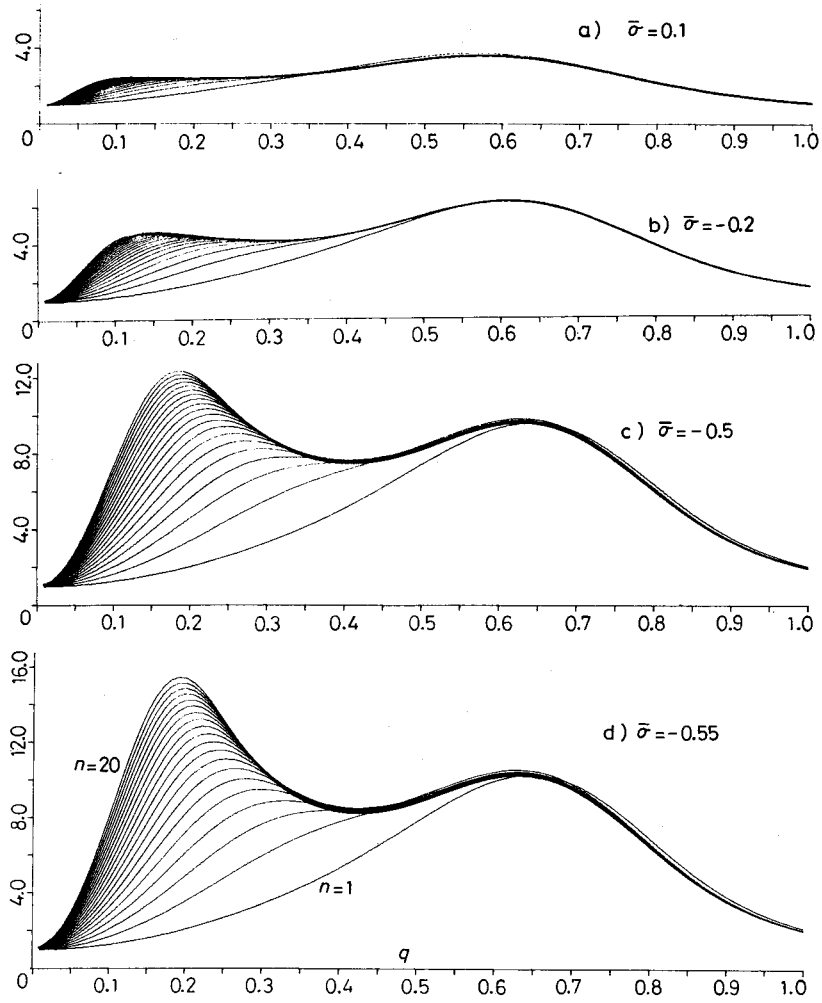

Fig. 4. $S_n(q)$ at $\mu=20$ for $\bar{\sigma}=\sigma-0.374=0.1,\ -0.2,\ -0.5,\ -0.55$. In these cases $\bar{\sigma}>\bar{\sigma}_c=-0.62$ and $S_n(q)$ tend to a limit which assumes the Ornstein-Zernike form for $q\lesssim\mu^{-1/2}$.

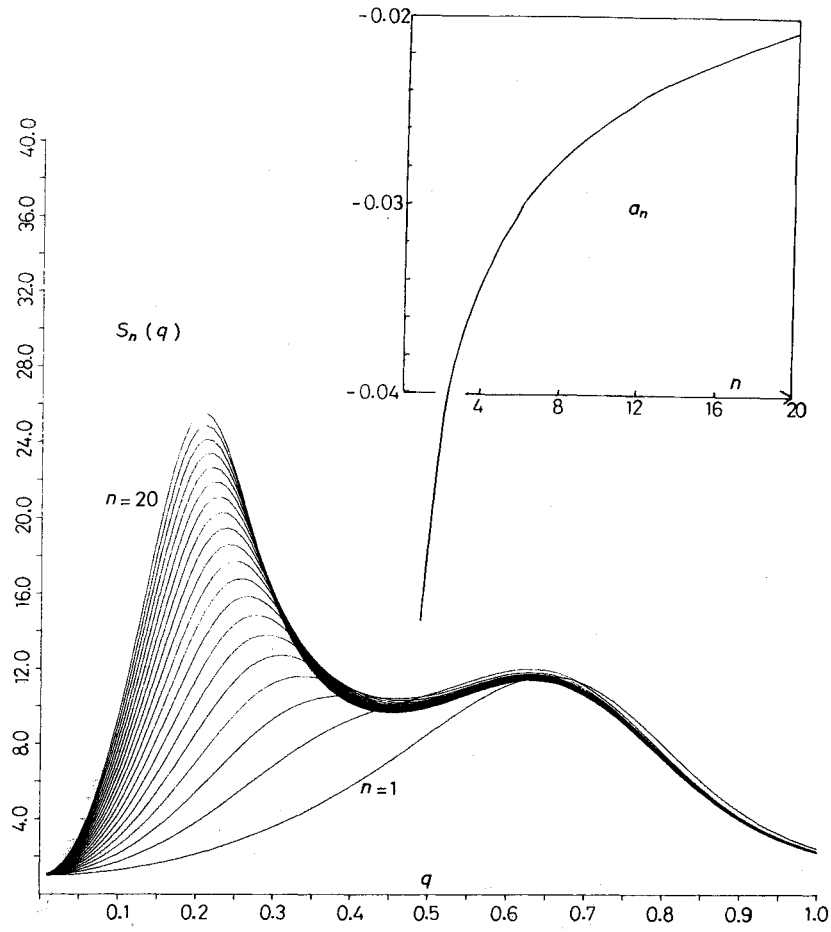

Fig. 5. $S_n(q)$ at $\mu=20$ and $\bar{\sigma}=-0.65$. Here a_n remain to be negative and the peak of $S_n(q)$ grows without limit as $n\to\infty$.

created and destroyed in each period, while the larger ones are created after several periods and do not change appreciably in one period. As σ is approached to σ_c, the sizes of the larger clusters become large. However, $S_n(q)$ have only one peak for short-time quenches ($\mu\lesssim 10$) or for shallow quenches ($\bar{\sigma}\gtrsim 0.2$). In the former case the effects of the oscillation are not strong. In the latter case the clusters created in each period are destroyed almost completely while $T>T_c$ and cannot grow furthermore.

The effective temperature $a(\tau)$ also behaves periodically as $\tau\to\infty$ for $\sigma>\sigma_c$. It is convenient to introduce its averages

$$a_n=\frac{1}{2\mu}\int_{2(n-1)\mu}^{2n\mu} d\tau a(\tau), \tag{3·4}$$

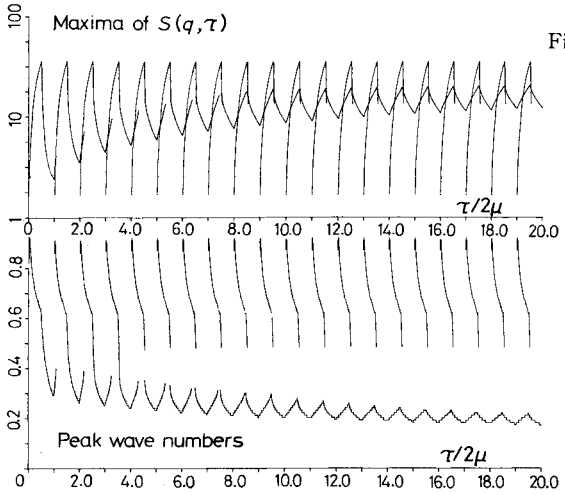

Fig. 6. (a) The two maximum intensities of $S(q, \tau)$ vs $\tau/2\mu$ at $\mu=20$ and $\bar{\sigma}=-0.55(>\bar{\sigma}_c)$ on a semi-log scale. The intensity at the larger wave number behaves periodically after several periods. It starts from 1.7, reaches the maximum 35.4, and decreases rapidly after reverse quench. The intensity at the smaller wave number is almost equal to $1/(q_m^2+a_\infty)$ where q_m is given by the lower curve of (b). (b) The wave numbers at which $S(q, \tau)$ has a peak. Their inverses represent the sizes of the two characteristic clusters. In the figure the smaller wave number q_m decreases as $\tau^{-1/4}$ (see the sentences below (3·9)).

which approach a positive number a_∞ for $\sigma>\sigma_c$. The values of σ_c and a_∞ are independent of the details of the initial conditions. For example, at $\mu=20$ and $\bar{\sigma}=\sigma-0.374=-0.55$, $a_{20}=0.01535$ for the initial conditions (3·1), whereas $a_{20}=0.01549$ if $S(q, 0)=(q^2+100)^{-1}$ and $b_1=b_2=v=0.01745$. The a_n appear to become a constant after several periods for $\sigma>\sigma_c$ and we expect $a_\infty\cong a_n$ for large n. In Fig. 7(a), a_{20} are shown as functions of $\bar{\sigma}$ for various μ. The values of σ at which $a_{20}=0$ are approximate values of σ_c.*) Note that the smaller of the two maximum wave numbers of $S_n(q)$, which will be denoted by q_m, is about $0.1\sim0.2$ at $n=20$ and shifts to lower values noticeably with the time scale of $q_m^{-4}=10^3\sim10^4$ at $\sigma\cong\sigma_c$. Hence it takes such long times to determine σ_c more precisely than the above method of $n=20$ as long as (3·1) is used. However, this difficulty can be overcome by rechoosing the initial conditions as those of the criticality $S(q,0)=1/q^2$, $b_1=b_2=0.3573$ and $v=0.2370$ and by setting $n=20$. In Fig. 7(b), the resultant values of σ_c are shown vs μ. The differences of these values and those at which $a_{20}=0$ with (3·1) are less than 0.05. We have found that σ_c goes to zero as $\mu\to0$. This is because the effects of the oscillation are negligibly small for small μ. In fact, we have checked that $S_n(q)$ at $\mu=1$ coincide with $S(q, \tau)$ for the non-oscillatory case (where $F(\tau/2\mu)$ is deleted in (2·14)) within 2% even at $n=20$.

Next we consider the long-time behavior of $S(q, \tau)$ for $\sigma>\sigma_c$. First we integrate (2·13) to obtain

$$S(q, 2n\mu+\tau)=U_q(2n\mu+\tau, 0)S(q, 0)+q^2\int_0^{2n\mu+\tau}d\tau' U_q(2n\mu+\tau, \tau'), \quad (3\cdot5)$$

*) In Ref. 4), σ_c was determined in this way.

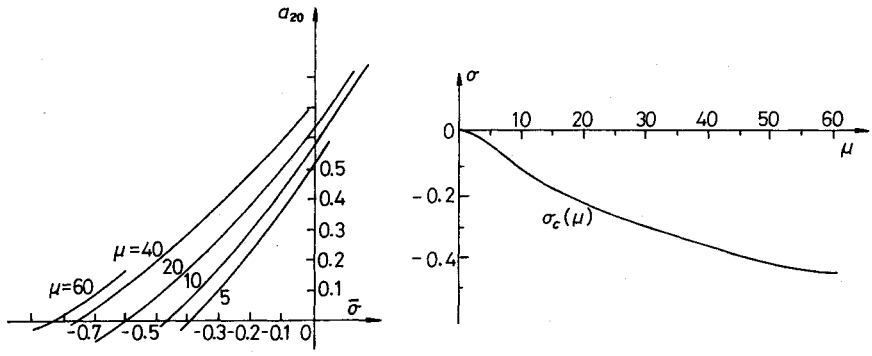

Fig. 7. (a) a_{20} vs σ for various μ. The values of $\sigma=\bar{\sigma}+0.374$ at which $a_{20}=0$ are slightly greater than σ_c. (b) σ_c vs μ. $\sigma_c\to 0$ as $\mu\to 0$ owing to the choice of r_{0c} (2·10). This curve is determined by setting $S(q,0)=1/q^2$.

where τ is chosen such that $0\leq\tau<2\mu$ and

$$U_q(\tau_1,\tau_2)=\exp[-q^2(q^2+a_\infty)(\tau_1-\tau_2)-q^2b(\tau_1)+q^2b(\tau_2)]. \tag{3·6}$$

The function $b(\tau)$ is defined by

$$b(\tau)=\int_{\tau_0}^{\tau}d\tau_1\, a(\tau_1)-(\tau-\tau_0)a_\infty, \tag{3·7}$$

which also tends to a periodic function as $\tau\to\infty$, τ_0 being an arbitrary time. As $n\to\infty$ the first term of (3·5) vanishes, and $S_\infty(q,\tau)\equiv\lim_{n\to\infty}S(q,2n\mu+\tau)$ becomes

$$\begin{aligned}S_\infty(q,\tau)&=q^2\int_0^\infty d\tau_1\, U_q(\tau,\tau-\tau_1)\\&=q^2[1-e^{-2\mu q^2(q^2+a_\infty)}]^{-1}\int_0^{2\mu}d\tau_1\, U_q(\tau,\tau-\tau_1),\end{aligned} \tag{3·8}$$

where $\tau_1=2n\mu+\tau-\tau'$ and use has been made of the fact that $b(\tau)$ is a periodic function at long times. On the second line of (3·8) the integration region $0<\tau_1<\infty$ has been divided into the intervals $2m\mu<\tau_1<2(m+1)\mu$ with $m=0,1\cdots$. In Fig. 8, $S_\infty(q,\tau)$ is shown at $\mu=20$ and $\bar{\sigma}=-0.2$ together with $S(q,40\mu+\tau)$ in the inset. For $q\gtrsim 0.2$ these two intensities coincide within a few percent. It is clear that the fluctuations with $\mu^{-1/2}\lesssim q\lesssim 1$ soon behave periodically after one or two periods and have the variance $S_\infty(q,\tau)$. This can be known from $|a(\tau)|\lesssim 1$ and $|b(\tau)|\lesssim\mu$.

On the other hand, the fluctuations with $q\lesssim\mu^{-1/2}$ can feel only the averages a_n

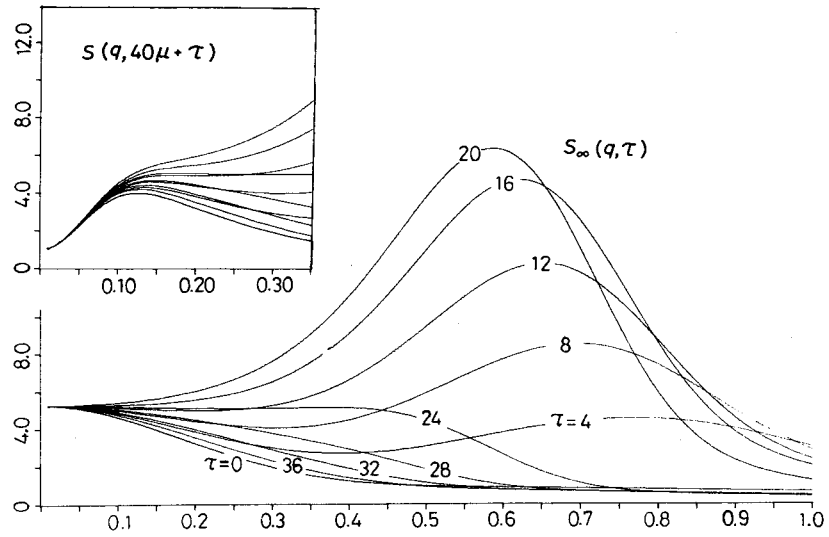

Fig. 8. $S_\infty(q,\tau)\equiv\lim_{n\to\infty} S(q, 2n\mu+\tau)$ at $\mu=20$ and $\bar{\sigma}=-0.2$. For $q\lesssim\mu^{-1/2}$ it is weakly dependent on τ and assumes the Ornstein-Zernike form, while for $q\gtrsim\mu^{-1/2}$ it oscillates rapidly corresponding to the periodic formation and annihilation of clusters. In the inset $S(q, 40\mu+\tau)$ is shown. These two intensities differ only at small wave numbers.

and their motion at long times can be simply described by

$$S(q,\tau)\cong\exp[-q^2(q^2+a_\infty)\tau]S(q,0)$$
$$+\{1-\exp[-q^2(q^2+a_\infty)\tau]\}(q^2+a_\infty)^{-1}. \qquad (3\cdot9)$$

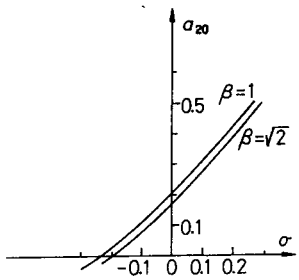

Fig. 9. Effect of changing the upper cutoff on a_{20} at $\mu=20$. The abscissa is σ, which is $\bar{\sigma}+0.374$ for $\beta=1$ and $\bar{\sigma}+0.565$ for $\beta=\sqrt{2}$.

Here $b(\tau)$ in (3·6) has been neglected by assuming that $q^2|b(\tau)|\sim\mu q^2\lesssim 1$. Therefore, $S(q,\tau)$ tends to the Ornstein-Zernike form $1/(q^2+a_\infty)$ for $q\lesssim\mu^{-1/2}$. The right-hand side of (3·9) has a peak at a wave number q_m if $a_\infty\ll 1$ and $S(q,0)\lesssim 1$. Here, q_m satisfies $q_m^2(q_m^2+a_\infty)\tau\sim 1$. Therefore, $q_m\sim(a_\infty\tau)^{-1/2}$ for $q_m\lesssim a_\infty^{1/2}$ and $q_m\sim\tau^{-1/4}$ for $a_\infty^{1/2}\lesssim q_m\lesssim(2\mu)^{-1/2}$.

Finally we show the effect of changing the upper cutoff $k_{\max}$. In Fig. 9 we display a_{20} vs σ for $\beta=1$ and $\sqrt{2}$ at $\mu=20$. The two curves agree well, but they differ considerably if plotted vs $\bar{\sigma}$. The cutoff dependence of $S(q,\tau)$ also becomes considerably weaker if it is regarded as

a function of σ (not as a function of $\bar{\sigma}$).

§ 4. Off-critical quench and spinodal curve

In this section we consider off-critical periodic quenches with $x_0 \neq 0$, where x_0 is defined by (2·16). As criticized by Binder et al.,[12),13)] the LBM theory does not take into account the nucleation process and results in an artificial spinodal curve. The validity of the theory is restricted to compositions close to the critical value. Because of this fact we give only a brief exposition of the calculations.

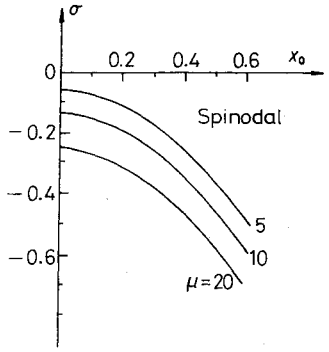

Fig. 10. $\sigma_c(\mu, x_0)$ vs x_0 for $\mu=5$, 10 and 20. These curves represent spinodals in the presence of the temperature vibration. The nucleation process is not accounted for in the calculation.

The behavior of $S_n(q)$ is similar to the case $x_0=0$. Namely, there is a critical value of σ, which is now dependent on μ and x_0 and will be written as $\sigma_c(\mu, x_0)$. For $\sigma > \sigma_c$, a_n tend to a positive limit, while for $\sigma < \sigma_c$ they remain negative. In Fig. 10 we plot $\sigma_c(\mu, x_0)$ for $x_0 \geq 0$. These curves represent the spinodal curves in the presence of the temperature vibration. They are approximately described by

$$\sigma_c(\mu, 0) - \sigma_c(\mu, x_0) \cong 1.125|x_0|^{1.75}. \tag{4·1}$$

The left-hand side is only weakly dependent on μ. The exponent 1.75 appears to be not important, because it changes to 1.95 for $\beta=\sqrt{2}$. Clearly, these spinodal curves are also artifacts of the approximation.

§ 5. Concluding remarks

Since the LBM theory is a decoupling approximation, it is inadequate in describing the motion of well-developed (or locally saturated) clusters within which the phase separation is locally completed and is also incapable of describing the nucleation and growth. Therefore, it is inapplicable to the late stage of the phase separation and to the off-critical case where the composition is not close to the critical value.

Consequently, our scheme for the periodic case is clearly inadequate when the dimensionless time interval μ is so long that the late stage of the phase separation is reached within the first period, and also when x_0, (2·16), is not close to zero.

We must also note that large saturated clusters may happen to be created by some "nucleation" process when σ is negative even at the critical composition.

Such clusters will not be well described by a self-consistent equation such as (2·6). They might grow indefinitely leading to the completion of the phase separation even for $\sigma > \sigma_c$. The effective temperature $A(\tau)$, (2·7), will be felt rather by plane-wave disturbances, so that σ_c calculated in this paper appears to correspond to the limit of metastability. Then the critical temperature will not be determined uniquely in experiments. These expectations suggest that the transition might be of first-order.

We also do not know the average composition after the separation (or the coexistence curve). It might jump discontinuously just below the transition which occurs as σ is lowered with μ fixed at a value much greater than unity.*) Note that the effect of the oscillation is considerably weaker in the off-critical case with x_0 not close to zero than in the critical case at the same average temperature. Namely, the effect of the oscillation will become weak after the separation, leading to some discontinuous change at the transition. This also suggests hysteresis behavior; that is, the system would behave differently depending on whether σ is approached to the critical value from the disordered phase or from the ordered phase.

The above statements are only conjectures at present.**) To confirm them we must examine the nucleation and growth (even at $x_0 = 0$). We must also remark that the results of this paper are not conclusive and may be inaccurate quantitatively. However, the main purpose of this paper is to present a new problem and propose new experiments.

Acknowledgements

The author would like to thank Professor K. Kawasaki, Professor W. I. Goldburg, Professor J. S. Langer and Professor J. W. Cahn for valuable discussions.

Appendix

The equation for $\bar{\rho}(y, \tau) \equiv (6/g)^{1/2} k_c \rho_1(c, t)$ will be expressed in the dimensionless units defined by (2·9) and (2·10). If $k_{\max} = \beta k_c$, it is of the form

$$\frac{\partial}{\partial \tau}\bar{\rho}(y, \tau) = A_0 \frac{\partial}{\partial y}\left[\frac{\partial}{\partial y} + g(y, \tau)\right]\bar{\rho}(y, \tau). \qquad (A \cdot 1)$$

Here,

*) For $\mu \ll 1$ the effect of the oscillation is weak and may be calculated by the linear response scheme. In this case the transition appears to remain of second order.

**) In the case of nonconserved order parameter the transition was shown to be of first-order within approximation schemes developed by Suzuki[14] and by Kawasaki, Yalabik and Gunton.[15]

$$A_0=(L\Delta/a^3{u_s}^2)/(2Lk_c{}^4)=(3/10)\beta^2 f_0{}^{-1}, \tag{A·2}$$

where $\Delta=(3/5)k_{\max}^2$, $a^3=6\pi^2/k_{\max}^3$, ${u_s}^2=(6/g)k_c{}^2$, and f_0 is related to $g^*\equiv g/k_c$ by

$$f_0=36\pi^2/(g^*\beta^3). \tag{A·3}$$

The function $g(y,\tau)$ is defined by

$$g(y,\tau)=(5/\beta^5)\bar{S}(\tau)y/\langle y^2\rangle + f_0[(y+x_0)^3-\langle(y+x_0)^3\rangle-\langle y(y+x_0)^3\rangle y/\langle y^2\rangle], \tag{A·4}$$

where

$$\bar{S}(\tau)=\int_0^\beta dqq^4[q^2+a(\tau)]S(q,\tau). \tag{A·5}$$

The equations of LBM reduce to the above equations if α and $\phi''(1)$ (in their notation) are replaced by $\beta/\sqrt{2}$ and 2, respectively.

Equation (A·1) will be solved by approximating the one-point distribution function as a sum of displaced Gaussians:

$$\bar{\rho}(y,\tau)=(2\pi)^{-1/2}v^{-1}(b_1+b_2)^{-1} \times\{b_2\exp[-(y-b_1)^2/2v^2]+b_1\exp[-(y+b_2)^2/2v^2]\}, \tag{A·6}$$

where b_1, b_2 and v are positive parameters. The second moment $\langle y^2\rangle=v^2+b_1b_2$ obeys

$$\frac{\partial}{\partial\tau}\langle y^2\rangle=2A_0-A_1\bar{S}, \tag{A·7}$$

where

$$A_1=3/(f_0\beta^3)=g^*/12\pi^2. \tag{A·8}$$

Equation (A·7) results in (2·9) if it is satisfied at $\tau=0$. We rewrite (2·9) in the dimensionless units:

$$\langle y^2\rangle=A_1\int_0^\beta dqq^2S(q,\tau). \tag{A·9}$$

The equations for $\langle y^3\rangle=b_1b_2(b_1-b_2)$ and $\langle y^4\rangle_c\equiv\langle y^4\rangle-3\langle y^2\rangle^2=b_1b_2[(b_1-b_2)^2-2b_1b_2]$ are given by

$$\frac{\partial}{\partial\tau}\langle y^3\rangle=-3A_0[5\beta^{-5}\bar{S}\langle y^3\rangle/\langle y^2\rangle+f_0(U_5+3x_0U_4)], \tag{A·10}$$

$$\frac{\partial}{\partial\tau}\langle y^4\rangle_c=-4A_0[5\beta^{-5}\bar{S}\langle y^4\rangle_c/\langle y^2\rangle+f_0(U_6+3x_0U_5)], \tag{A·11}$$

where $U_4=\langle y^4\rangle-\langle y^2\rangle^2-\langle y^3\rangle^2/\langle y^2\rangle$, $U_5=\langle y^5\rangle-\langle y^3\rangle\langle y^2\rangle/\langle y^2\rangle$, and $U_6=\langle y^6\rangle-\langle y^3\rangle^2-\langle y^4\rangle^2/\langle y^2\rangle$.

Equations (A·7), (A·10), (A·11) and (2·13) constitute a closed set of equa-

tions. In these equations the temperature $r(t)$ appears only in $a(t)=A(t)/k_c^2$ and hence the LBM scheme is capable of straightforward generalization to arbitrary $r(t)$. The desired equations can be readily obtained if the scale of wave numbers k_c and the cut-off wave number k_{max} are specified. We give some possible examples in the following:

i) The LBM choice: $r+r_{0c}=-x^2$, $k_c=x$, and $k_{max}=\sqrt{2}ax$. Here

$$a(\tau)=A(t)/k_c^2=-1+\langle(y+x_0)^3y\rangle/\langle y^2\rangle. \qquad (A\cdot12)$$

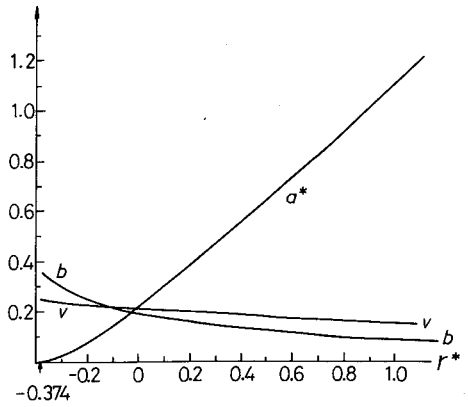

Fig. 11. a^*, $b(=b_1=b_2)$, and v vs $r^*=(r+r_{0c})/k_c^2$ in stationary states of the LBM model at $x_0=0$ and $k_c=k_{max}$.

If $|x_0|$ is smaller than a particular value x_{0c}, $a(\tau)$ remains negative and $S(q,\tau)$ grows without limit. However, if $|x_0|$ is greater than x_{0c}, $a(\tau)$ tends to a limit $a_\infty(\geq 0)$ as $\tau\to\infty$ and $S(q,\tau)$ also tends to $(q^2+a_\infty)^{-1}$. Thus $c_0=\pm(6/g^*)^{1/2}\,xx_{0c}$ represents a spinodal curve in the LBM approximation. This spinodal is, however, an artifact of the approximation, as was stressed by Binder et al. In fact, x_{0c} is found numerically to decrease with increasing a as $x_{0c}=0.73$, 0.59, 0.46 for $a=0.8$, 1.0, 1.2, respectively.

ii) $a^*=\lim_{\tau\to\infty} a(\tau)\geq 0$, $r=$const, $x_0=0$, and $k_{max}=k_c$. We are considering a stationary state of the LBM model at the critical composition. In Fig. 11 we plot a^* vs $r^*=(r+r_{0c})/k_c^2$. The limit a^* vanishes at $r^*=r_{0c}^*=-0.374$.

iii) If $r(t)$ is oscillating as (1·3), we find (2·14).

References

1) A. Onuki, Prog. Theor. Phys. **66** (1981), 1230.
2) A. Onuki, Prog. Theor. Phys. **67** (1982), 768.
3) A. Onuki, Prog. Theor. Phys. **67** (1982), 787.
4) A. Onuki, Phys. Rev. Letters **48** (1982), 753.
5) J. W. Cahn, Acta Metall. **9** (1961), 975; **10** (1962), 179.
6) J. W. Cahn, Trans. Metall. Soc. AIME **242**(1968), 166.
7) J. E.Hillard, in *Phase Transformation*, edited by H. I. Aronson (American Society of Metals, Metals Park, Ohio, 1970).
8) See for example, J. Marro, J. L. Lebowitz and M. H. Kalos, Phys. Rev. Letters **43** (1979), 282.
9) P. C. Hohenberg and B. I. Halperin, Rev. Mod. Phys. **49** (1977), 435.
10) J. L. Langer, M. Bar-on and H. D. Miller, Phys. Rev. **11A** (1975), 1417.
11) K. Kawasaki and T. Ohta, Prog. Theor. Phys. **59** (1978), 362.
12) K. Binder, C. Billotet and P. Mirold, Z. Phys. **B30** (1978), 183.
13) K. Binder, in *Lecture Notes in Physics 132*, (Springer-Verlag, 1980).
14) M. Suzuki, Advances in Chemical Physics **46** (1981), 195.
15) K. Kawasaki, M. C. Yalabik and J. D. Gunton, Phys. Rev. **A17** (1978), 455.